Soft Matter

Cite this: *Soft Matter*, 2011, **7**, 5020

www.rsc.org/softmatter

PAPER

A neutron reflectivity study of the interfacial and thermal behaviour of surface-attached hairpin DNA†

Tanja H. M. Kjällman,[a] Andrew Nelson,[b] Michael James,[bc] Joseph A. Dura,[d] Jadranka Travas-Sejdic*[ae] and Duncan J. McGillivray[f]

Received 8th November 2010, Accepted 1st March 2011
DOI: 10.1039/c0sm01284j

Mixed self-assembled monolayers (mSAMs) have been successfully utilised as platforms for gene sensors, employing optical as well as electrochemical means of detection. Probe density is one of the most important parameters in the construction of such a sensor and thus a fundamental understanding of the structure within the mSAM is vital. In this work, the interfacial behaviour of mixed SAMs, where short PEG oligomers co-adsorbed to the surface with hairpin structured oligonucleotide (ODN) probes, has been investigated. The neutron reflectivity of the mixed SAMs was measured at differing HPP : PEG ratios, and through two routes of formation, to elucidate the effect of controlled HPP surface density on surface conformation of the probes and on the final hybridised ODN–HPP construct. General conclusions regarding the structure of the investigated SAMs could be drawn from determined thickness and volume fraction values and conformational changes in the mSAM, induced by hybridisation with complementary ODN, were also detected. An investigation of the melting behaviour of the surface-attached HPPs was also conducted with polarised neutron reflectivity and clear signs of melting were observed in the reflectivity and the SLD profiles around 45 °C.

Introduction

Molecular beacons (MBs) are single stranded nucleic acid probes, which in the absence of their target strands form hairpin-like secondary structures. The actual probe sequence is situated in the loop part of the strand and the stem is formed by base-pairing the two complementary arm sequences at either side of the loop. Traditionally, a fluorescent molecule is attached to one end of the probe, whereas a quencher is attached to the other end and in the non-hybridised state the MB is in a "dark" state. The naturally adopted hairpin structure undergoes a thermodynamically driven conformational change upon hybridisation with its complementary strand, forming a double-stranded DNA helix and forcing the fluorescent marker away from the quencher, resulting in a "bright" state.[1,2] Tyagi and Kramer were the first to employ MBs in a solution assay for the detection of DNA hybridisation and found that MBs showed great ability to distinguish even single-base mismatches from their complementary target sequence,[2] thus rendering them suitable probes for sequence-specific detection of their targets. The hairpin secondary structure can also be utilised as a probe without the fluorescent label and the quencher and thus the probe used here is referred to as a hairpin probe (HPP) instead of a molecular beacon.

Additionally, HPPs have been adapted to surface-immobilised systems, which rely on optical as well as electrochemical means of signal detection.[3,4] As various thioalkanes and thioalcohols[5–7] have been used for creating a mixed monolayer as a sensing platform it has been shown that control of the surface density of the probes in these monolayers is crucial if sensitive and selective sensors are to be achieved.[3,4,6–8] In order to construct such an efficient and well-designed sensing platform, a deep understanding of the structure within the mSAM is required. Characterisation of mixed self-assembled monolayers (mSAMs), based on short poly(ethylene glycol) (PEG) molecules and hairpin probes (HPPs), was attempted with techniques such as ATR-FTIR and high-resolution tapping-mode

[a]*Polymer Electronic Research Centre, The University of Auckland, Private Bag 92019, Auckland, New Zealand. E-mail: tanja.kjallman@gmail.com; j.travas-sejdic@auckland.ac.nz; Fax: +64 9 373 7499; Tel: +64 9 373 7599*
[b]*Bragg Institute, Australian Nuclear Science and Technology Organisation, Building 87, Locked Bag 2001, Kirrawee DC, NSW, 2232, Australia*
[c]*School of Chemistry, University of New South Wales, Kensington, NSW, 2052, Australia*
[d]*NIST Center for Neutron Research, National Institute of Standards and Technology, 100 Bureau Drive, Gaithersburg, MD, 20899, USA*
[e]*The MacDiarmid Institute for Advanced Materials and Nanotechnology, New Zealand*
[f]*Department of Chemistry, The University of Auckland, Private Bag 92019, Auckland, New Zealand*
† Electronic supplementary information (ESI) available. See DOI: 10.1039/c0sm01284j

AFM. Neither of these methods could fully characterise and describe the system, which has been shown to be a functional platform for a sensitive and selective DNA sensor.[9] NR has been shown to successfully probe soft samples, such as membranes and thin films, on solid surfaces and provide information about the density and the thickness of the studied layer[10–12] and was thus selected for characterisation of mixed PEG : HPP SAMs, before and after hybridisation with target ODN.

In 1998 a pioneering neutron reflectivity (NR) study on self-assembled DNA monolayers on gold was published by Levicky *et al.*[13] The conformational changes of the surface-tethered ss-DNA were studied as a result of 6-mercapto-1-hexanol (MCH) treatment, followed by hybridisation. NR was determined to be a valuable technique for this study because it enabled depth-profiling with Ångström-level resolution.[13] Concentration profiles for the samples were obtained and the ss-DNAs were observed to pass from a compact to an extended configuration upon MCH treatment. The authors concluded that control of the monolayer formation was achieved and that the ss-DNAs were terminally tethered to the gold surface. Upon hybridisation the ds-DNA strands were found to position themselves towards the normal of the substrate, increasing the thickness of the monolayer.[13]

Recently, Steichen *et al.*[14] reported on the interfacial behaviour of a hairpin DNA probe, which was co-immobilised on gold with a short thiol (mercaptobutanol). They followed the conformational change of unlabelled hairpin probes, as they unfolded from a closed hairpin structure to form rigid double strands when hybridised with complementary targets. The NR data confirmed that the conformational change increased the DNA layer thickness on the gold substrate,[14] in a more marked transformation for the HPPs than that previously observed for a layer based on ss-DNA.[13]

This work extends previous work by measuring the interfacial behaviour of mixed SAMs in which short PEG oligomers were co-adsorbed to the surface with HPPs in differing HPP : PEG ratios, and through two routes of formation (co-assembly or step-wise assembly on the surface). Our previous work has already shown that this has a significant effect on sensitivity of the HPP as a DNA sensor.[9] This work probes the effect of controlled HPP surface density on surface conformation of the probes and on the hybridised DNA–HPP construct.

Polarised neutron reflectometry (PNR) was also employed to measure the melting behaviour of the surface-attached HPPs, for a comparison with the melting profiles obtained for HPPs in solution. Polarised neutron reflectometry (PNR) measures the neutron spin-dependent reflectivity, and relies on the presence of a magnetic layer, such as Fe, within the substrate. A sufficiently strong applied magnetic field causes the reference layer to magnetically align with it, such that two effective SLD densities are measured by the neutrons—one in which the neutron spin is aligned parallel to the magnetic field and one in which the neutrons are aligned anti-parallel.[12,15] Two independent sets of data are thus obtained from a single sample without any additional sample preparation,[16] which is particularly advantageous for easily perturbed biological samples or when *in situ* experiments are conducted.

Experimental

Materials‡

The oligonucleotide (ODN) probe 5′-HS-C_6H_{12}-ACA CGC TCA TCA AGC TTT AAC TCA TAG TGA GCG TGT-3′, complementary target 5′-ACG CTC ACT ATG AGT TAA AGC TTG-3′ were purchased from Alpha DNA, Canada. Thiolated mPEG [H_3C–$(CH_2CH_2O)_6CH_2CH_2SH$] was purchased from Polypure (Norway). 0.01 mol L^{-1} PBS buffer (0.0027 mol L^{-1} KCl and 0.137 mol L^{-1} NaCl) was prepared using Milli-Q water (18.2 Ω cm resistivity), and was used as a solvent for all HPP immobilisation and hybridisation. Deuterated water (D_2O), Milli-Q H_2O and a 1 : 1 mixture of D_2O and Milli-Q H_2O (CM 2.5) with a neutron scattering length density (SLD) of 2.5×10^{-6} $Å^{-2}$ were used as solvents for the neutron measurements. Gold-coated silicon wafers were used as substrates for the NR and PNR measurements, prepared at the National Institute of Standards and Technology (NIST) Center for Nanoscale Science and Technology (CNST), USA. The wafers had a diameter of 75 mm and a thickness of 5 mm, and were coated with approximately 30 Å of Cr (NR) or Fe (PNR) and 150 Å of gold. These were contained in a temperature controlled aluminium cell, containing a 300 μL solvent reservoir next to the sample surface.

Pretreatment of Au-coated Si-wafers and mixed monolayer preparation—NR

The gold-coated wafers were rinsed with ethanol prior to SAM formation. Two immobilisation strategies were used: (1) immobilisation of the gold surface with HPPs, followed by addition of PEG molecules and (2) simultaneous self-assembly of probes and PEG from a mixture containing a predetermined molar ratio of the two components. The self-assembly of probes and/or PEG on the gold surface was done by flowing 3 mL of a solution with a predetermined probe and/or PEG concentration, through the assembled cell. For immobilisation strategy (1), the probe (HPP) solution (4.65 μmol L^{-1}) was pumped first through the cell at a rate of 3 mL h^{-1} for 1 h, at room temperature. The surface was rinsed thoroughly with PBS buffer to remove any unattached HPPs, followed by back-filling with PEG, deposited in the same manner (flow rate and time) as the probe but with a PEG concentration of 46.5 μmol L^{-1}. The mixed SAM (mSAM) surface was then thoroughly rinsed again with PBS buffer to remove any remaining unattached PEG molecules. A similar deposition procedure was used for immobilisation strategy (2) but molar ratios of PEG : HPP (2 : 1 and 10 : 1) were used for simultaneous immobilisation for 1 h at room temperature. Surfaces were thoroughly washed to remove any unattached molecules before neutron measurements were made.

‡ *Note*: certain commercial materials, equipment, and instruments are identified in this paper in order to specify the experimental procedure as completely as possible. In no case does such identification imply a recommendation or endorsement by the National Institute of Standards and Technology, nor does it imply that the materials, equipment, or instruments identified are necessarily the best available for the purpose

Pretreatment of Au-coated Si-wafers and mixed monolayer preparation—PNR

The HPPs were initially immobilised for 1 h, rinsed and measured, and then immobilisation was continued for an additional hour to enhance the density of the probes. After mSAM was formed the surface was thoroughly rinsed and PNR data had been collected at 22 °C, the temperature was raised stepwise and data were acquired at selected temperatures of 35, 45, 55 and 65 °C. The temperature was allowed to stabilize for at least 10 min before each measurement.

Hybridisation-NR

Hybridisation was carried out by flowing 6 mL of a 4.65 μmol L^{-1} complementary target solution through the assembled cell at a flow rate of 5 mL h^{-1} using a syringe pump. The temperature was kept at 37 °C. After hybridisation the surface was thoroughly rinsed with PBS buffer to remove any non-hybridised target DNA before neutron reflection data were collected.

Hybridisation-PNR

Hybridisation was carried out by flowing 3 mL of a 4.65 μmol L^{-1} complementary target solution through the assembled cell over an hour. The temperature was kept at 35 °C. After hybridisation the surface was thoroughly rinsed with PBS buffer to remove any non-hybridised target DNA and PNR before data were collected at 35 °C.

Neutron reflectometry

NR was carried out on the Platypus reflectometer, at the Bragg Institute, Australian Nuclear Science and Technology Organisation (ANSTO) in Sydney, Australia.[17] Data were collected from the reflected beam at three different angles of incidence: 0.5°, 2.0° and 6.0°, corresponding to a maximum momentum transfer of $Q_z = 0.4$ Å^{-1} (4 nm^{-1}), with each full measurement taking approximately 4 hours. A minimum of two solvents (with different SLDs) were used (H_2O-, and D_2O-based 10 mmol L^{-1} PBS buffer with a pH of 7.4) for all samples, with the addition of a CM 2.5 contrast (1 : 1H_2O : D_2O/PBS buffer) when possible within the experimental timeframe. Reduction and initial analysis of the data was done with the software *Motofit*[18] written for Igor Pro 6.04 (Wavemetrics).

Polarised neutron reflectometry

PNR was carried out at the NG-1 reflectometer at NIST Center for Neutron Research, Washington DC, USA.[19] Data were collected up to a maximum momentum transfer of $Q_z = 0.3$ Å^{-1} (3 nm^{-1}) using a polarised neutron beam to obtain two magnetic contrasts (from the different neutron spin states interaction with an embedded magnetised Fe layer). The two polarised contrasts were measured simultaneously, and the complete Q-range was measured in 8 hours. Measurements were predominantly made in a D_2O/PBS buffer, but also in H_2O/PBS buffer (10 mmol L^{-1}, pH 7.4). Reduction and initial analysis of the data was done using the NIST software suite *Reflpak*.[20]

(P)NR data analysis

All relevant datasets were fitted simultaneously during the analysis with the program ga_refl.[20] The structure of the sample was determined by fitting the experimental data to a layer composition model which included the thickness, the SLD and the roughness of the different layers. The parameters of the Si/SiO_2/Cr/Au or Si/SiO_2Fe/Au wafers were initially characterised to obtain the thickness and the SLD of the substrate layers and the values attained were fixed for subsequent fitting. The amount of water present (and consequently the amount of DNA) in the mSAM can be estimated through the following relation:

$$\rho_{\text{HPP-layer}} = vf_{\text{solv}}\rho_{\text{solv}} + (1 - vf_{\text{solv}})\rho_{\text{DNA}} \quad (1)$$

where $\rho_{\text{HPP-layer}}$, ρ_{solv} and ρ_{DNA} are the SLD values of the HPP-layer, of the solvent and of DNA, respectively, and vf_{solv} is the volume fraction of the solvent in the layer. Eqn (1) thus gives the density of the total layer, under the assumption that it contains only HPP and solvent in it (*i.e.*, that $vf_{\text{HPP}} = 1 - vf_{\text{solv}}$).

Results and discussion

Characterisation of mSAMs before and after hybridisation with complementary DNA

SAMs with different densities of PEG : HPPs as well as reference samples with only PEG or HPP monolayers were studied with NR. Specifically, four different monolayers, consisting of: (1) only PEG molecules, (2) only HPPs, (3) the HPP-only sample subsequently backfilled with PEG and (4) simultaneously immobilised PEG : HPPs with the molar ratio 2 : 1, were investigated. PEG was used to displace any un-specifically attached HPPs. The general experimental design (NR and PNR) is shown in Scheme 1.

The theoretical fully extended length of a PEG molecule, with six repeat units, is 2.5 nm[10] and the height of the HPP is estimated to be 4–5 nm. The double stranded DNA, which forms during hybridisation, has a fully extended length of 13 nm, and thus the thickness of the monolayer was expected to alter upon hybridisation with complementary target DNA, providing a detectable change in the surface properties. The layer thickness of the pure PEG layer was calculated to be 1.6 nm, with a volume fraction of

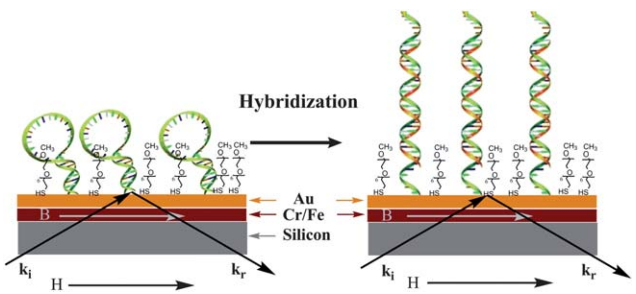

Scheme 1 A schematic (not to scale) illustration of the experiment performed with polarised neutron reflectometry. For NR experiments at ANSTO, Cr was used as the adhesive layer between silicon and gold, whereas Fe was used in PNR experiments to achieve magnetic contrast. H represents the external and B the internal magnetic fields applied in PNR.

50.1% (Fig. S1, ESI†), less than the maximum of 2.5 nm. This can be explained by considering the short PEG molecules to be inclined to the surface normal—it has been shown that self-assembled alkanethiols on gold have an average tilt of ~30° from the surface normal.[21] Ehler *et al.*[22] found tilt angles around 40° for alkanethiols, with a methylene chain length of 11–19 units, on gold. The shortest chains ($n = 11$) exhibited the largest tilt (45°), which the authors attributed to polycrystallinity in the surface structure.[22] The tilt angle of the PEG SAM investigated in this study was calculated to be around 50°, greater than for a densely packed alkanethiol layer,[21,22] and consistent with a reported tilt-angle of 50° for moderately sparse layers of $C_{18}H_{37}SH$ alkanethiols on Au (111) surfaces.[23] This information, together with the high solvent volume fraction, suggests that the short immobilisation time has resulted in a low density layer of PEG on the Au surface. Nevertheless, a sharp transition from the PEG layer to the solvent layer was observed in the SLD profile for the PEG SAM (Fig. S2, ESI†) indicating a homogeneous PEG-layer (modelled parameters are in Table 1).

The second reference layer investigated contained only HPPs, which was subsequently backfilled with PEG molecules and hybridised with cODN for 1 h at 37 °C. The reflectivity data for these three samples are displayed in Fig. 1, where the experimental data are represented by markers and the fitted curves are shown as solid lines. The corresponding modelled SLD profiles are presented in Fig. 2. The HPP-only layer gave rise to a measured thickness of 2.0 nm and a volume fraction of 7.7% (Fig. 1A and 2, dotted lines). Based on the obtained layer thickness and volume fraction and the coverage of HPPs on the Au surface the average density corresponded to 1.5×10^{12} HPP molecules cm^{-2}. This is lower than the density of single-stranded probes determined by Levicky *et al.* (approx. 6×10^{12} chains cm^{-2} for single-stranded probes),[13] which is influenced by the short immobilisation time as well as the fact that the HPP has a double stranded structure at the stem region where it binds to the gold surface, increasing the surface occupied by each probe.

The low thickness of the HPP layer, which is of the same magnitude as the diameter of a double stranded DNA helix,[24] suggests that the HPPs were positioned flat on the Au rather than extending into the solvent. This is consistent with previous reports, in that the absence of spacers (such as MCH or PEG), DNA adsorbs non-specifically to gold.[13,25] Given the less dense layer that is formed for the HPPs than for the PEG and the greater length of the HPP, it stands within reason that the calculated tilt angle (68°) is higher for the HPP than the PEG-layer. However, it is important to bear in mind that all the values obtained are averages over the sample area studied. Horizontal resolution is restricted with NR, which is sensitive to changes normal to the substrate surface. Thus, all the measured data and the calculated tilt angles are averages over a distribution of behaviours, from molecules normal to the surface to those more or less lying down.

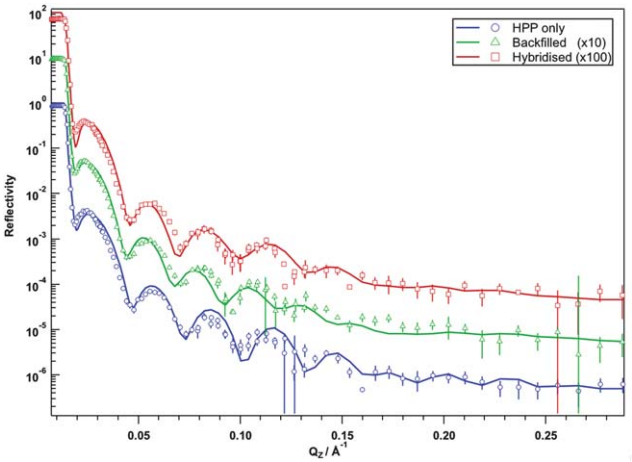

Fig. 1 The reflectivity profiles for samples measured in D_2O PBS buffer of: a monolayer containing only HPPs (blue circles), the same layer after backfilling with PEG (green triangles), and after hybridisation with complementary target ODN at 37 °C for 1 h (red squares). The solid lines are derived from the fitted models. Three different contrasts, D_2O, CM 2.5 and H_2O, were used in the modelling for the HPP only measurements, while two contrasts, D_2O and H_2O, were used for the successive measurements (other contrasts not shown). The reflectivity profiles are offset by a factor 10 for clarity.

When the HPP layer was backfilled with PEG (Fig. 1B and 2, dotted-solid lines) a two-layer structural model for the fits was required to account for separation of the PEG and HPPs or dsODN layer. Upon backfilling with PEG, there was an increase in both the layer thickness and the non-solvent volume fraction, from 2 nm to a total of 2.7 nm and from 7.7% to a total of 25%, respectively—indicating an increase in the surface coverage. This transformation is visible in the SLD profile (Fig. 2), particularly the D_2O contrast, when the backfilled HPP layer (dotted-solid lines) is compared to the HPP layer (dotted lines). These results suggest that the PEG molecules are able to reduce non-specific adsorption between DNA and Au and prop up immobilised DNA into a more upright position,

Table 1 Summary of layer thickness and volume fraction values for the investigated SAMs, derived from a 2-layer model fit of the reflectivity data (Platypus, ANSTO)

2-Layer model (except for PEG and HPP only[a])	1st layer thickness/nm	1st layer volume fraction (%)	2nd layer thickness/nm	2nd layer volume fraction (%)	Total thickness above Au/nm	Total volume fraction above Au (%)
PEG only	1.6 (0.1)	50 (5)	—	—	1.6 (0.1)	50 (5)
HPP only	2.0 (0.1)	7.7 (0.8)	—	—	2.0 (0.1)	7.7 (0.8)
HPP + backfill PEG	2.5 (0.2)	23 (2)	0.2 (0.1)	0.8 (0.1)	2.7 (0.2)	25 (2)
HPP + backfill PEG hybridised	6.7 (0.6)	7.6 (0.8)	0.5 (0.1)	0.5 (0.1)	7.2 (0.7)	8.1 (0.9)
2 : 1 PEG : HPP	2.1 (0.1)	20 (2)	1.9 (0.1)	0.2 (0.1)	4.0 (0.2)	20 (2)
2 : 1 PEG : HPP hybridised	1.1 (0.1)	34 (3)	3.0 (0.2)	0.3 (0.1)	4.1 (0.3)	34 (3)
10 : 1 PEG : HPP	1.0 (0.1)	23 (2)	4.2 (0.4)	9.9 (1)	5.2 (0.5)	32 (3)

[a] A 1-layer model was applied for the PEG- and HPP-only SAMs. Estimated uncertainties are shown in brackets.

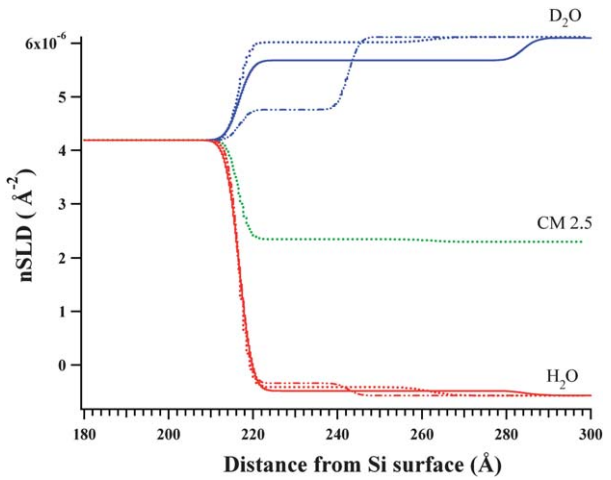

Fig. 2 The neutron SLD profiles for a monolayer of only HPPs (dotted lines), after backfilling with PEG (dotted-solid lines) and after hybridisation (solid lines) with complementary target ODN at 37 °C for 1 h. Three different contrasts, D_2O (blue lines), CM 2.5 (green line) and H_2O (red lines), were used for the measurements of the pure HPP layer, whereas two contrasts, D_2O and H_2O, were used for the backfilled- and the hybridised layers.

consistent with previous findings regarding various thioalkanes[3,4,6–8,25] and further supported by the decrease in the attained tilt angle from 68° to 61°. The large tilt angle even after backfilling can partially be explained by the presence of the C_6-linker at the 5′-end of the probe sequence. The length of the linker is approximately the same as the thickness of the PEG molecules, and the more the rigid stem of the HPPs protrudes from the PEG-layer the more rotational freedom they attain.

After hybridisation with cODN further alterations were distinguishable in the SLD profiles (Fig. 1C and 2, solid lines, respectively). The total thickness of the two layers in the model increased further to 5.1 nm while the total non-solvent volume fraction decreased to 12%. These results indicate that hybridisation induces an increase in the layer thickness, as expected, although the modelled thickness implies that the HPP/target duplexes were still not arranged normal to the substrate, but at a tilt angle of 56°. Thiolated fifteen base-paired duplexes have been shown to tilt at about 45° when self-assembled on gold.[26] The HPP/target duplexes formed in this study are longer and have a more flexible unpaired stem than the fifteen-based duplexes investigated by Kelley *et al.*[26] and therefore a larger tilt-angle is not unexpected. A higher penetration of solvent into the layer closest to the substrate is seen by the decrease in the non-solvent volume fraction and the loss of definition between the mixed layer containing PEG/HPP and the outer layer containing only HPP/ODN. This indicates that the hybridisation process bares a part of the substrate surface that has previously been covered by the hairpin structure. On hybridisation of the loop section of the probe with complement DNA the double stranded stem of the original HPP is separated to form a ssDNA section, with the result that DNA is removed from the near-surface PEG-layer. The reduction in the amount of material in the layer nearest to the surface, and the simultaneous increase in the amount of material above the mixed PEG/DNA layer, reduces the density contrast between the two layers such that they are no longer well-defined separate entities. It can be assumed that the increase in the amount of detected material can be attributed to the attachment of target ODN. Using this assumption, the surface coverage after hybridisation of the backfilled layer was estimated to be 5.8×10^{12} HPP molecules cm^{-2} and the estimated density of bound cODN in the backfilled layer corresponded to 0.76×10^{12} HPP molecules per cm^{-2}.

These results can be directly compared to the work of Steichen *et al.* This group also investigated the structural change of a DNA hairpin occurring after hybridisation but they concentrated solely on a 1 : 1 (molar ratio) HPP : 4-mercaptobutan-1-ol (MCB) layer.[14] The HPP concentration before hybridisation was reported as 7.2×10^{12} HPP molecules cm^{-2}. Their surface coverage is higher than the HPP only layer studied here, which was 1.5×10^{12} HPP molecules cm^{-2}, a natural result of the much longer mSAM assembly time (>16 h) used by Steichen *et al.* Nevertheless, the change of thickness of surface structure on hybridisation was very similar for the two systems—a 4 nm increase for the HPP/MCB,[14] and 4.5 nm for the backfilled HPP-layer here.

It has been shown that probe density is a critical factor in the construction of efficient DNA sensors[27,28] and consequently mSAMs with various HPP concentrations, controlled by co-adsorption with differing ratios of PEG, were investigated. Fig. 3 shows the SLD profile for a mSAM with a molar ratio of PEG : HPP 2 : 1 before and after hybridisation with cODN (for 1 h at 37 °C). Modelling gave a total thickness of 4.0 nm and a 20% volume fraction for the PEG : HPP layer above the substrate before hybridisation. From the estimated tilt angle of 48° and the sharp transition in the SLD profile (Fig. 3, dotted lines) it can be concluded that the PEG : HPP 2 : 1 SAM forms a denser layer with the components in a more upright position than the backfilled layer.

The surface coverage was estimated as up to a maximum 7.9×10^{12} HPP molecules cm^{-2}, as the PEG molecules are included but not separately accounted for in the HPP layer (as the SLD difference between the PEG and HPP was too small to separately resolve the two components within the resolution of the

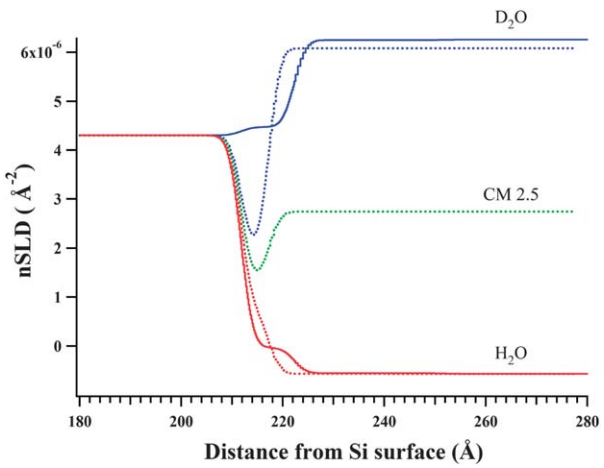

Fig. 3 The neutron SLD profile for the PEG : HPP 2 : 1 mSAM before (dotted lines) and after (solid lines) hybridisation with complementary target ODN at 37 °C for 1 h. The data were collected at three different contrasts: D_2O (blue lines), CM 2.5 (green line) and H_2O (red lines).

experiment). The surface coverage of up to 7.9×10^{12} HPP molecules cm^{-2} is comparable to the surface coverage of the PEG-backfilled HPP layer before hybridisation (6.6×10^{12} HPP molecules cm^{-2}), the slightly higher value reflecting the longer immobilisation time, and similar to the 7.2×10^{12} mol cm^{-2}, reported by Steichen *et al.*[14] After the cODN was introduced (Fig. 3, solid lines) the change in the total thickness of the mSAM was insignificant. However, the volume fraction increased from 20 to 35% suggesting that the target did bind to probe sequence in the HPP, with an increase in surface coverage estimated to be 1.4×10^{12} HPP molecules cm^{-2}. The amount of bound ODN was thus found to be 6.1×10^{12} HPP molecules cm^{-2}, indicating that the PEG : HPP mSAM was more efficient as a DNA sensor than the backfilled HPP-layer. This result is in agreement with the electrochemical response we have determined previously for a similar HPP-based DNA sensor.[9]

At the extreme level of dilution a simultaneously immobilised layer of PEG : HPP with a molar ratio of PEG : HPP 10 : 1 was measured after immobilisation for 1 h at room temperature (Fig. S3 and S4†). A total thickness of 5.7 nm was observed, with a volume fraction of 33%, and an estimated tilt angle was 19°. Simultaneous immobilisation of the two components in the mSAM yields a thicker and denser layer compared to the back-filling strategy presented in Fig. 1B and 2 (dotted-solid lines). This result is in accordance with previously acquired AFM-data, which showed that the RMS-value for the PEG : HPP 10 : 1 layer was higher than the PEG : HPP 2 : 1 layer, indicating that the latter ratio produced a smoother and denser layer (results not shown). The major features in the reflectivity and SLD-profiles for the PEG : HPP 10 : 1 layer (Fig. S3 and S4†, respectively) arose from the PEG molecules but the contribution of the HPPs could be seen in comparison between the SLD-profile of a pure PEG-layer (Fig. S2†) with the PEG : HPP 10 : 1 layer. The SLD of PEG is not as close to that of the solvents as the SLD of the PEG : HPP 10 : 1-layer, which is a clear indication of the presence of the HPPs. Also, the thickness of a sole PEG-layer was calculated to be 1.6 nm, whereas the PEG : HPP 10 : 1 mSAM had a 1st layer, predominantly representing the PEG molecules, of only 1 nm. Although the formation of the PEG : HPP 10 : 1 mSAM was observed, the density of the HPPs on the surface proved to be so low that they were on the detection limit of the instrument, and thus hybridisation studies were not modelled.

Table 1 summarises the detailed layer thicknesses and volume fractions for all the investigated layers, derived from the 2-layer model fit of the reflectivity data. For the two mSAM samples—backfilled HPP and PEG : HPP 2 : 1—the 2-layer model showed similar thickness and volume fractions for the first layer (closer to the substrate), 2.5 *versus* 2.1 nm and 24 *versus* 20%, respectively, before hybridisation. The thickness of the second layer, considered to contain the fractions of the HPP structures that were longer than the PEG-molecule, was very thin (~0.2 nm) with a volume fraction of less than 1%.

After hybridisation both the thickness and the volume fraction decreased in the first layer, while the opposite was seen for the second layer. This is in accordance with the hypotheses that when the HPPs unfold in the presence of their complementary targets part of the substrate is bared, demonstrated as a decrease in material of the first layer as part of the stem is removed, but as an increase in the second layer as the target is bound to the probe. The same trend was observed for the mSAM consisting of PEG : HPP in a 2 : 1 ratio, except for an increased volume fraction observed in both the first and the second layer after hybridisation. The greater amount of material in the first layer is related to the more upright position of the initial mSAM, where the HPP/target duplex was partially extended down into the first layer. The formation of a mSAM with an even lower probe density was also detected, although it was close to the detection limit of the instrument. In order to validate the 2-layer model of the mSAM more experiments are needed, preferably with polarised neutrons, as the inclusion of magnetic contrast is likely to reduce model ambiguity.

Polarised neutron reflectometry for investigation of the melting behaviour of the surface-attached probes in the mSAM

Sterical constraints due to the high probe density in the sensing layer have been shown to affect the hybridisation efficiency.[27,28] If the hybridisation temperature is increased, close to the melting point of the HPP, these constraints can be overcome,[9] although the details of structural transformations near the melting point of the HPP are unknown. PNR was employed to investigate the melting profile of the surface attached HPPs. Preliminary determination of the melting temperatures of unbound oligonucleotides (ODNs) (both probes and duplexes) in solution has been carried out by detecting the change in UV-absorbance with increasing temperature (results not shown). However, these results on DNA in solution can only be seen as an indication of the melting temperature of the surface attached HPPs. The temperature dependent behaviour of surface attached ODNs is not well known, and the unfolding of the HPPs in particular is difficult to detect with other techniques (such as Surface Plasmon Resonance) as it does not involve any mass changes. Electrochemical techniques have to some extent been used to measure the melting of single-stranded probes and their targets,[29–31] but we are unaware of NR being previously employed to probe the melting of surface-bound DNA, especially HPPs. Using NR it was possible to simultaneously determine the melting temperature, and the conformational changes of the DNA-probe during the hybridisation process. The unfolded and fully extended probe has an approximate maximum height of 13 nm,[32] and thus a significant change in the thickness of the monolayer upon increasing the temperature above the melting point of the hairpin is expected even if the HPP does not adopt a fully extended conformation. The magnetic contrast method, using polarised neutrons, was necessary for these samples to allow contrast change at elevated temperatures without disturbing the delicate hairpin probe system, as would be necessary using solvent contrast. Due to time restrictions and the efforts involved in obtaining beam time at neutron sources, the results presented here are indicative only and further melting studies of the surface-attached probes should be conducted to elucidate the exact melting temperature.

To ensure a sufficient amount of HPP present at the surface, the HPPs were immobilised for 2 h with a ten-fold higher solution concentration of HPPs than for the previous HPP-only study. The surface coverage of the formed layer was estimated to be 7.1×10^{12} HPP molecules cm^{-2}, with a volume fraction of 60% (Table 2). These results indicate that a SAM of HPP was formed

Table 2 Summary of layer thickness and volume fraction values, at different temperatures or after hybridization, for a HPP SAM, derived from a 1-layer model fit of the polarized neutron reflectivity data (NG-1 reflectometer, NCNR). Estimated uncertainties are shown in brackets

1-Layer model	Thickness/nm	Volume fraction (%)
HPP only, 1 h, 22 °C	1.2 (0.1)	45 (5)
HPP only, 2 h, 22 °C	1.2 (0.1)	60 (6)
HPP (2 h), 37 °C	2.0 (0.1)	87 (4)
HPP (2 h), 45 °C	1.5 (0.1)	94 (5)
HPP (2 h), 55 °C	2.7 (0.2)	47 (5)
HPP (2 h), 65 °C	1.9 (0.1)	23 (2)
HPP (2 h) + cODN, 22 °C	2.6 (0.2)	18 (2)

on the Au surface in close vicinity of the Au layer, at a significantly higher density than that observed for the earlier HPP-only surface studied. The HPP layer created after 2 h of immobilisation showed a thickness of only 1.2 nm, which indicates that once again the majority of the HPPs are lying flat on the Au surface, with non-specific adsorption occurring between the HPPs and the Au.[8,13,25]

To investigate the melting behaviour of surface-attached HPPs, neutron reflection was measured at five different temperatures: 22, 35, 45, 55 and 65 °C, covering the expected HPP melting point range. 22 °C corresponds to standard room temperature, 35 °C is in the range of common hybridisation temperatures, 45 °C is close to the calculated (44.7 °C) and experimentally determined (47.1 ± 0.4 °C) melting temperatures for the HPP-4 in solution (results not shown), and 55 °C and 65 °C were chosen expecting fully dissociated HPPs. Only data obtained with the up spin neutrons are presented here, although all data have been included in the modelling, even when not explicitly shown.

The reflectivity profile for one spin of the polarised neutron measurements of the HPP layer at different temperatures is displayed in Fig. 4. The SLD profiles for the HPP layer at different temperatures were calculated based on the fitted reflectivity data and the up-spin profiles are shown in Fig. 5. The changes in the HPP layer, due to the increase in temperature, are highlighted by the narrowed *x*-axis range and all the layer thicknesses and volume fractions acquired from the model are summarised in

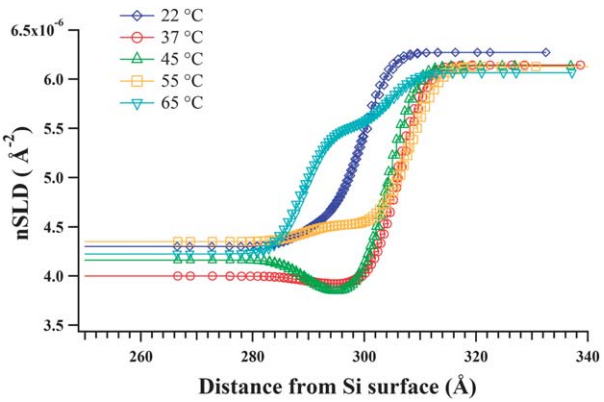

Fig. 5 Neutron SLD profile for up-spin magnetic contrasts of a HPP SAM measured at 5 different temperatures: 22 °C (blue diamond line), 35 °C (red dot line), 45 °C (green triangle line), 55 °C (orange square line) and 65 °C (light blue inverted triangle line). The data were acquired in a D_2O environment.

Table 2. At room temperature (22 °C) the HPPs are expected to be in their stem-loop conformation[33,34] and thus the data acquired at that temperature are used as reference points for the subsequent measurements.

Hybridisations are typically carried out at 37 °C, which corresponds to the biological temperature at which DNA naturally undergoes the hybridisation process in the human body.[24] The temperature regulation for the experimental setup was difficult and a monitoring of the temperature during the measurement showed (35 ± 1) °C, although the aim was 37 °C. In Fig. 5 a shift in the SLD profile is seen at 35 °C (red line), compared to the reference profile at 22 °C (blue diamond line), due to an increased thickness and volume fraction of the HPP layer from 1.2 to 2.0 nm and from 60 to 87%, respectively (Table 2). The immobilisation of the HPPs is a spontaneous process and thus the layer formed is likely to be heterogeneous, especially at lower temperatures and short immobilisation times. The increase in layer thickness and volume fraction at 35 °C indicates that the HPPs covered most of the Au substrate, possibly due to an alignment of the HPPs to achieve a more

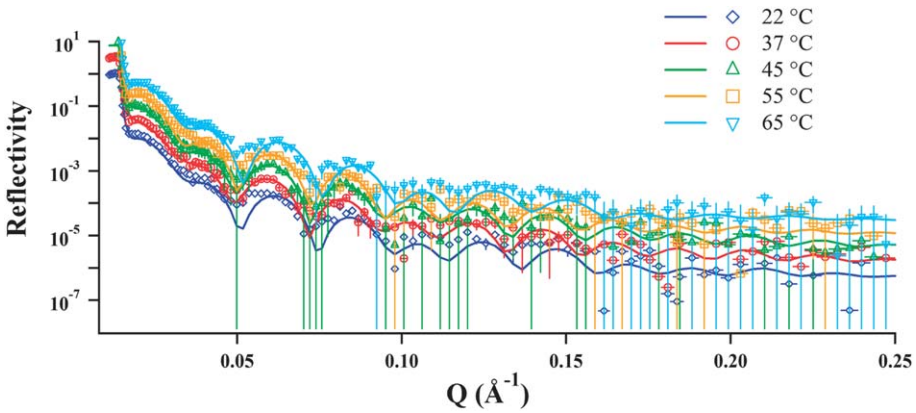

Fig. 4 Neutron reflectivity profile for up-spin magnetic contrasts of a HPP SAM measured at 5 different temperatures: 22 °C (blue diamond), 35 °C (red circle), 45 °C (green triangle), 55 °C (orange square) and 65 °C (light blue inverted triangle). The markers represent the data and the solid lines represent the fits. The data were acquired in a D_2O buffer and are offset on the *y*-axis, with respect to the 22 °C dataset, for clarity.

homogenous layer with less electrostatic repulsion between the negatively charged HPPs. That reduction of the non-specific adsorption between the ODN backbone and the substrate would account for the increased thickness was ruled out because non-thiolated DNA reportedly adsorbs so strongly to a flat Au surface that it cannot be removed by either extensive rinsing with buffer or water, or heating the gold surface to 75 °C.[25]

When the temperature was elevated further to 45 °C the shape of the SLD profile changed slightly (Fig. 5, green triangle line) and the slope steepened somewhat. The HPP-layer shrunk slightly in terms of thickness, likely due to a change in configuration from rigid HPPs to random coils.[34] However, the almost complete coverage of the Au surface was achieved as determined by the volume fraction of 94% (Table 2). As the temperature intervals in this study were quite wide and clear differences can be noted between the SLD profiles at the various temperatures, the exact melting temperature of the surface-attached HPPs is difficult to determine based solely on these results.

It is tempting to propose a melting temperature in the vicinity of 45 °C (since the volume fraction is very high at that temperature) which would be surprisingly close to the simulated T_m of 44.7 and the experimentally determined T_m of 47.1 for HPP-4 in solution (results not shown). As the base pairs in the stem of the HPP become destabilised and the hydrogen bonds start to break the HPPs become more mobile and thus free to interact with neighbouring HPPs. Importantly, stems from different destabilised HPPs might even base pair into new "stems" (double-stranded regions), affecting the layer arrangement. Brewood *et al.* reported a T_m of 62.0 °C for hairpins attached to gold interdigitated microelectrode (GIME).[29] The authors found that same hairpin in solution had a T_m of 47.8 °C (predicted T_m above 40 °C), which is in agreement with previous studies,[30,31] where it has been showed that attachment to a surface stabilises DNA strands and thus increases the T_m. The results presented here do not show clear signs of a stabilising effect due to the surface-attachment of the HPPs. This disagreement could be accounted for by the differences in the hairpin structures themselves. The HPP consists of a 9-base pair long stem with 18 bases in the loop, whereas the HPP used by Brewood *et al.* consisted of a 20-base pair long stem with only 4 bases in the loop.[29] Although both HPPs exhibited similar T_m in solution, the greater length of the stem in the HPPs attached to the interdigitated microelectrodes would indeed enhance the stability of the HPPs compared to the shorter stem HPPs. Additionally, the buffer used by Brewood *et al.*[29] contained a higher salt concentration, which contributed to the stabilisation of the HPP and, consequently, to a higher T_m.[25,33] A relatively low T_m of the HPP would be supported by the electrochemical response for a DNA sensor based on mSAM of HPP and PEG molecules as a hybridisation temperature of 44 °C has been found advantageous (compared to hybridisation at 37 °C) especially for high probe density mSAMs.[9]

However, at 55 °C a more pronounced change in the SLD profile (Fig. 5, orange square line) can be distinguished. This can be explained as the volume fraction of HPPs on the surface decreases significantly from 94 to 47% while the thickness of the layer increases from 1.5 nm to 2.7 nm (Table 2). At this temperature the HPPs are likely to be released from their original structure and exist in a random coil configuration,[34] *i.e.*, they behave like highly flexible single stranded probes and thus a larger fraction of the solvent was entwined with the probes, similarly to the volume fraction observed at 22 °C. The major differences in the layer at 22 °C, compared to 55 °C, are the structural conformation of the HPPs on the surface, as seen in Fig. 5, the orange square line. As discussed previously, at 22 °C the HPPs are likely to lie flat on the surface, in rigid stem-loop structures, whereas at higher temperatures enhanced conformational freedom allows for a larger variety within the layer[33,34] and allow part of the random coils to protrude into the solvent layer, observed an increase in layer thickness.

When the temperature was raised to 65 °C the SLD profile changed further, as shown in Fig. 5, light blue inverted triangle line. As listed in Table 2, there was a notable decrease in the layer thickness and also a loss of material on the surface as the volume fraction of HPP was reduced from 47 to 23%. It has been shown that a thiol–Au bond can be broken by the application of a fs-long laser pulse.[35] The laser pulse led to the desorption of thiolated DNA strands from a Au nanoparticle surface, observed through changes in the nanoparticle surface plasmon absorption band.[35] More recently, Herdt *et al.* investigated the integrity of the thiol–Au bond for Au–DNA conjugates when exposed to high temperatures.[36] Gold particles were functionalised with ODNs, tagged with fluorophores, and the dissociation of the thiolated DNA–Au bond was characterised over time with fluorescence measurements, gel electrophoresis and ion-exchange chromatography.[36] It was found that, above 70 °C, there were two reasons for the decomposition of the aqueous Au–DNA conjugates: (1) desorption of thiol-terminated DNA from the gold nanoparticle surface and (2) chemical degradation of DNA in the presence of colloidal gold.[36] Since the substrate used in this study for immobilisation of the HPPs was not of colloidal character, and the temperature was not raised above 65 °C during the measurements (due to current set-up restrictions), a degradation of the ODN strand itself was unlikely. However, an indication of partial thiol–Au bond dissociation could be observed as a clear change in the SLD profile (Fig. 4, orange line) at 65 °C and as the substantial decrease in volume fraction (from 47 to 23%), as listed in Table 2. In order to determine the T_m for the surface-attached HPPs, smaller temperature intervals should be used and both the heating up and cooling down should be monitored.

After the temperature profile was measured the HPP SAM was cooled down to room temperature and subsequently hybridised with cODN at 35 °C. The SLD profiles revealed a condition dependent conformational change for the HPPs (Fig. S5†). A volume fraction of only 18% for the hybridised layer (Table 2) provides support for the assumption that the thiol–Au bonds have partially been broken during the previous melting profile measurements. If all HPPs had remained bound to Au substrate through their thiol groups, a volume fraction similar to, or larger than, that of the HPP layer before any treatment (~60%, Table 2) would have been expected after hybridisation with cODN. The volume fraction was, however, notably reduced suggesting that 65 °C was enough to weaken the thiol–Au bonds sufficiently to detach a number of the HPPs.

The thickness of the hybridised layer, 2.6 nm, was similar to the 2.7 nm measured for the non-hybridised layer of HPPs at

55 °C, in support of the view that the HPPs protrude into the solvent layer at 55 °C. The SLD profile (Fig. S5†) for the hybridised duplex exhibited some similar characteristics with the random coil HPP-layer but shows a more marked difference between the solvent and the ODN layer, suggesting that the hybridised layer was denser and more rigid than the random coil, as expected. However, a fully extended hybridised HPP/target complex has an approximate height of 10–13 nm, which is far from the measured 2.1 nm. As previously mentioned, the diameter of a double helix is about 2 nm and thus it can tentatively be concluded that the double strands were lying down on the Au surface, instead of positioning themselves in a position normal to the surface. This observation is supported by consideration of the non-specific adsorption of the pyrimidine and purine bases in the duplex to the Au surface,[25] the presence of a C_6-linker between the thiol group and the first base at the 5′-end of the HPP and the low amount of ODNs present on the Au substrate. It is possible that the C_6-linker increased the flexibility of the HPP/target duplex close to the surface so that the adsorption of the nitrogen rich bases to the Au surface was strong enough to position the hybridised strands horizontally on the substrate.

Conclusions

Neutron reflectometry was used for the characterisation of mSAMs of PEG and/or HPPs to gain insight of the composition of the formed layers. General conclusions regarding the structure of the investigated SAMs can be drawn from thickness and volume fraction values, determined from the model fit. Conformational changes in the mSAM, induced by hybridisation with cODN, were also detected. All the studied SAMs exhibited layer thicknesses that were smaller than expected, based on the maximum theoretical heights of the participating molecules, suggesting that the SAMs are not densely packed on the surface allowing molecule conformations tilted away from the surface normal. The precise distribution of the HPPs (*versus* the PEG molecules) could not be determined, although some information concerning the densities of the mSAMs was obtained. The surface coverage before melting was found to be 7.1×10^{12} HPP molecules per cm^{-2}. Further measurements are needed in order to confirm the results obtained in this study, but important preliminary information about the nature of the structure of the mSAMs was gained through neutron reflection measurements.

An early exploration of the melting behaviour of the HPP was also conducted by means of polarised neutron reflectometry. Magnetic contrasts are achieved by changing the spin of the neutrons used and this enhances the contrast variation in a simple and straightforward way, without any intrusion on the sample. Although the temperature intervals employed were rather wide, there were clear signs of melting in the reflectivity and the SLD profiles around 45 °C. These results showed that the melting temperature for the surface-attached HPPs is remarkably close to 47.1 °C, which was the T_m measured for same HPP in solution. In order to establish a more thorough understanding of the thermodynamic behaviour of the immobilised HPPs further experiments are needed, focusing especially on the region between 40 and 50 °C.

Acknowledgements

The authors thank the Australian Institute of Nuclear Science and Engineering (AINSE), the Marsden Fund of the Royal Society of New Zealand and the MacDiarmid Institute for Advanced Materials and Nanotechnology for financial support, and the NIST Center for Nanoscale Science and Technology for access to equipment. TK is grateful to the staff of the Bragg Institute for the help during the Platypus reflectometer commissioning. DJM gratefully acknowledges support from an AINSE Research Fellowship.

References

1 B. Dubertret, M. Calame and A. J. Libchaber, *Nat. Biotechnol.*, 2001, **19**(4), 365–370.
2 S. Tyagi and F. R. Kramer, *Nat. Biotechnol.*, 1996, **14**(3), 303–308.
3 H. Du, C. M. Strohsahl, J. Camera, B. L. Miller and T. D. Krauss, *J. Am. Chem. Soc.*, 2005, **127**(21), 7932–7940.
4 Y. Xu, L. Yang, X. Ye, P. He and Y. Fang, *Electroanalysis*, 2006, **18**(9), 873–881.
5 C. Fan, K. W. Plaxco and A. J. Heeger, *Proc. Natl. Acad. Sci. U. S. A.*, 2003, **100**(16), 9134–9137.
6 R. Lao, S. Song, H. Wu, L. Wang, Z. Zhang, L. He and C. Fan, *Anal. Chem.*, 2005, **77**(19), 6475–6480.
7 S. Pan and L. Rothberg, *Langmuir*, 2005, **21**(3), 1022–1027.
8 H. Du, M. D. Disney, B. L. Miller and T. D. Krauss, *J. Am. Chem. Soc.*, 2003, **125**(14), 4012–4013.
9 T. H. M. Kjallman, H. Peng, C. Soeller and J. Travas-Sejdic, *Anal. Chem.*, 2008, **80**(24), 9460–9466.
10 S. A. Holt, A. P. Le Brun, C. F. Majkrzak, D. J. McGillivray, F. Heinrich, M. Loesche and J. H. Lakey, *Soft Matter*, 2009, **5**(13), 2576–2586.
11 S. Krueger, C. W. Meuse, C. F. Majkrzak, J. A. Dura, N. F. Berk, M. Tarek and A. L. Plant, *Langmuir*, 2001, **17**(2), 511–521.
12 J. Penfold and R. K. Thomas, *J. Phys.: Condens. Matter*, 1990, **2**(6), 1369–1412.
13 R. Levicky, T. M. Herne, M. J. Tarlov and S. K. Satija, *J. Am. Chem. Soc.*, 1998, **120**(38), 9787–9792.
14 M. Steichen, N. Brouette, C. Buess-Herman, G. Fragneto and M. Sferrazza, *Langmuir*, 2009, **25**(7), 4162–4167.
15 C. F. Majkrzak, *Physica B*, 1991, **173**(1–2), 75–88.
16 C. F. Majkrzak and N. F. Berk, *Physica B*, 1999, **267–268**, 168–174.
17 M. James, A. Nelson, S. A. Holt, T. Saerbeck, W. A. Hamilton and F. Klose, *Nucl. Instrum. Methods Phys. Res., Sect. A*, 2011, **632**, 112–123.
18 A. Nelson, *J. Appl. Crystallogr.*, 2006, **39**, 273–276.
19 J. A. Dura, D. J. Pierce, C. F. Majkrzak, N. C. Maliszewskyj, D. J. McGillivray, M. Losche, K. V. O'Donovan, M. Mihailescu, U. Perez-Salas, D. L. Worcester and S. H. White, *Rev. Sci. Instrum.*, 2006, **77**, 074301.
20 P. A. Kienzle, M. Doucet, D. J. McGillivray, K. V. O'Donovan, N. F. Berk and C. F. Majkrzak, *ga_refl: Flexible Reflectometry Modelling Software*, 2000–2009.
21 A. B. Horn, D. A. Russell, L. J. Shorthouse and T. R. E. Simpson, *J. Chem. Soc., Faraday Trans.*, 1996, **92**(23), 4759–4762.
22 T. T. Ehler, N. Malmberg and L. J. Noe, *J. Phys. Chem. B*, 1997, **101**(8), 1268–1272.
23 E. Barrena, C. Ocal and M. Salmeron, *J. Chem. Phys.*, 2001, **114**(9), 4210–4214.
24 L. Stryer, *Biochemistry*, W.H. Freeman and Company, New York, 4th edn, 1995, p. 1064.
25 T. M. Herne and M. J. Tarlov, *J. Am. Chem. Soc.*, 1997, **119**(38), 8916–8920.
26 S. O. Kelley, J. K. Barton, N. M. Jackson, L. D. McPherson, A. B. Potter, E. M. Spain, M. J. Allen and M. G. Hill, *Langmuir*, 1998, **14**(24), 6781–6784.
27 F. Ricci, R. Y. Lai, A. J. Heeger, K. W. Plaxco and J. J. Sumner, *Langmuir*, 2007, **23**(12), 6827–6834.
28 J. Zhang, S. Song, L. Zhang, L. Wang, H. Wu, D. Pan and C. Fan, *J. Am. Chem. Soc.*, 2006, **128**(26), 8575–8580.
29 G. P. Brewood, Y. Rangineni, D. J. Fish, A. S. Bhandiwad, D. R. Evans, R. Solanki and A. S. Benight, *Nucleic Acids Res.*, 2008, **36**(15), e98.

30 E. Finot, E. Bourillot, R. Meunier-Prest, Y. Lacroute, G. Legay, M. Cherkaoui-Malki, N. Latruffe, O. Siri, P. Braunstein and A. Dereux, *Ultramicroscopy*, 2003, **97**(1–4), 441–449.
31 R. Meunier-Prest, S. Raveau, E. Finot, G. Legay, M. Cherkaoui-Malki and N. Latruffe, *Nucleic Acids Res.*, 2003, **31**(23), e150/1–e150/8.
32 B. Tinland, A. Pluen, J. Sturm and G. Weill, *Macromolecules*, 1997, **30**(19), 5763–5765.
33 G. Bonnet, O. Krichevsky and A. Libchaber, *Proc. Natl. Acad. Sci. U. S. A.*, 1998, **95**(15), 8602–8606.
34 G. Bonnet, S. Tyagi, A. Libchaber and F. R. Kramer, *Proc. Natl. Acad. Sci. U. S. A.*, 1999, **96**(11), 6171–6176.
35 K. P. Jain, W. Qian and M. A. El-Sayed, *J. Am. Chem. Soc.*, 2006, **128**, 2426–2433.
36 A. R. Herdt, S. M. Drawz, Y. Kang and T. A. Taton, *Colloids Surf., B*, 2006, **51**(2), 130–139.